Reconstitution of *Drosophila* fertilization for time-lapse imaging

Júlia Pereira Nunes[1,2]
[1] Instituto Superior Técnico, Technical University of Lisbon, Lisbon, Portugal
[2] Instituto Gulbenkian de Ciência, Oeiras, Portugal

Abstract

Insect fertilization starts with sperm entry at the anterior side of the egg through a protrusion called micropyle. Following sperm activation and the formation of the paternal pronucleus, it is thought that a coordinated displacement of both paternal and maternal pronuclei within the cytoplasm leads to pronuclear apposition and the first mitotic division. However, the sequence of events and the causality have been deduced from fixed and immunostained samples. Thus, we lack relevant temporal and dynamics information. Because fertilization happens deep inside the egg, which is carried inside a living organism and filled with diffractive yolk, any state-of-art time-lapse light microscopy has been challenging. The main goal of this project was to develop a reconstitution assay of *Drosophila melanogaster* fertilization enabling live microscopy. This implied the design of an *ex vivo* experimental approach in which a female pronucleus in a single droplet of cytoplasm is fertilized with a single sperm cell, and in which both pronuclei and the associated cytoskeleton can be observed live at high resolution. To this end, eggs were harvested with precisely determined timing of female meiosis. *In vivo* imaging of non-fertilized eggs allowed to observe female meiosis completion. This knowledge will set the basis for the cytoplasmic isolation of the female pronucleus. Finally, it was possible to perform time-lapse imaging of pronuclear apposition and mitosis in the extract from recently fertilized eggs. This novel assay opens new avenues to study chromosomal dynamics during fertilization enabling more detailed insight, for example, into bacteria transmission and cytoplasmic incompatibility.

Keywords: *Drosophila melanogaster*, Fertilization, Meiosis, Microscopy, Pronuclei

I. INTRODUCTION

In *Drosophila melanogaster (Dmel)*, female meiosis is resumed during egg activation (Heifetz, Yu, and Wolfner 2001; Page and Orr-Weaver 1997). Meiosis completion leads to the formation of the female pronucleus, which locates deep in the cytoplasm of the egg. (Riparbelli and Callaini 1996). The sperm-egg interaction mediates the fertilization of the egg by one single sperm cell (Perotti 1975). Subsequently, sperm activation drives the formation of a functional male pronucleus in order to initiate pronuclear apposition. As parental chromosomes appose, the bipolar apparatus is assembled by the centrosomes inherited from the sperm cell (Callaini and Riparbelli 1996; Sonnenblick

1950). The first mitosis marks the beginning of the syncytial embryo development (Foe and Alberts 1983; Zalokar and Erk 1976). Despite the interest in the study of the *Dmel* zygote, the earliest stages of embryogenesis are largely understudied. Several technical difficulties, including the fact that the egg is a large structure filled with diffractive particles, have limited live imaging of subcellular events during fertilization. Therefore, most of our knowledge about *Dmel* fertilization has been derived from fixed and immunostained samples. Existing evidence has only allowed to represent fertilization as a fragmented process based on a hypothetical chronological order of morphological snapshots (Fitch and Yasuda 1997). Thus, it is lacking relevant spatiotemporal information and correlation of underlying processes. The absence of a suitable methodology for live imaging of recently fertilized eggs has been a major drawback for the study of cellular, structural and biochemical events taking place upon fertilization. Here, it is described the development of an assay allowing *ex vivo* reconstitution of *Dmel* fertilization for high-resolution time-lapse imaging.

Conceptually, a single embryo extract assay (Telley et al. 2013) was adapted and several procedural modifications were introduced. The same procedure for egg preparation was adopted, however with different egg laying schedule, for *in vivo* imaging of non-fertilized eggs. Initial experiments allowed real time visualization and temporal annotation of transitions during meiosis completion in naturally activated eggs, which were then compared with previous studies of *in vitro* activated eggs (Endow and Komma 1997). In order to reconstitute fertilization, both *in vivo* and *ex vivo* conditions were combined with live microscopy allowing time-lapse visualization of pronuclear apposition and the first mitotic nuclear division. Once optimized, this methodology will be a useful tool for the study of chromosomal dynamics in *Wolbachia* infected flies.

II. METHODS

1. Fly strains and crosses

Fly stocks were raised at 25ºC on standard corn meal food in 60 ml plastic containers. A strain expressing the MAP4 variant Jupiter tagged with GFP (Jup::GFP) was used to report microtubule structures, and the histone 2A variant tagged with RFP (H2Av::RFP) as a chromosomal marker in a wild-type background (w^{1118}). These fluorescent tags enabled the visualization of microtubules and chromatin dynamics inside both non-fertilized and fertilized eggs as well as in the egg extract. Infertile males were generated by crossing wild-type (w^{1118}) virgin with males of transgenic line carrying X and Y compound chromosomes (Bloomington stock no.82). The progeny of this cross included fertile females and infertile males; males were then selected for the egg-laying assay. The seminal vesicle (SV) was extracted from male flies expressing the beta–tubulin variant tagged with GFP (β–tub::GFP) as a microtubule marker in a wild-type background (w^{1118}). This transgenic fly strain produced fluorescence at high enough

contrast allowing detection of the sperm tail inside an egg.

2. Microscopy system setup

All mechanical manipulations and image acquisitions were performed on an Andor spinning-disk confocal microscope equipped with custom-made extensions. The system was composed of a Nikon Eclipse Ti-E inverted microscope coupled to a Yokogawa CSU-W1 spinning disk confocal scanner, four excitation laser lines (405, 488, 561, 640 nm), and two different cameras: a Zyla 4.2 sCMOS (6.5 µm pixel size) and an iXon3 888 EM-CCD (13 µm pixel size), connected to TuCam (all Andor). The nosepiece was equipped with 10x Plan 0.25 NA, 20x Plan Fluor 0.75 NA, 40X Plan Fluor 1.30 NA and 60X Apo TIRF 1.49 NA objective lenses. The Nikon XY stage carried a 220-µm piezo Z-stage for rapid 3D acquisition. The built-in extraction setup included micropipette-based fluidic devices mounted directly to the microscope stand. A static platform hosted four 3-axis micromanipulators connected to XYZ micro-controllers. Micro-capillaries and micro-cantilevers facilitated the extraction or manipulation, respectively, of specimen such as the egg or the male SV. One pipette holder was connected to a syringe pump whose activity was controlled by foot-pedals. Time-lapse image acquisition was accomplished with the software iQ3 (Andor), which also controlled the excitation laser intensity, the exposure time of the cameras and the position of the XYZ microscope stage. Different imaging protocols were created to acquire time-resolved confocal single plane or Z-stack images using GFP and RFP excitation.

3. Egg collection and sample preparation

The collection and preparation of both non-fertilized and fertilized eggs was adopted from an earlier protocol established for embryo extraction (Telley et al. 2013), with a few procedural modifications. Fly cages standing on agar plates supplemented with fresh yeast paste were used to perform a general egg-laying assay. For non-fertilized egg collection, fly cages were set up with ~60 virgin females alone or in the presence of ~25 infertile males. Egg synchronization was performed by replacing the agar plate every 15-20 minutes. The final egg collection did not exceed 10 minutes. For fertilized egg collection, fly cages were set up with ~60 virgin females and ~30 males. For this condition, egg laying was synchronized by replacing the agar plate every 10 minutes and egg collection did not exceed 7 minutes. Default egg treatment included dechorionation followed by immobilization in one row on a PLL-treated glass coverslip, and coverage with halocarbon oil.

4. Single egg extract assay

Initial sample focusing was performed in bright-field mode using a 10x objective. Evaluation of the developmental stage for each egg was conducted using confocal fluorescence microscopy at 20x and 40x magnification using GFP and RFP excitation. Each laser line was adjusted to the optimal power to maximize signal and minimize

phototoxicity effects. For extraction, the microscope was switched to transmission mode, and under visual inspection through the ocular both vitelline and plasma membranes of the posterior end were punctured with a crude pipette followed by aspiration of cytoplasm into the pipette. Once 30–50% of the embryo volume was extracted, the microscope stage was moved so that the field of view showed a clean glass surface. Small droplets of cytoplasm (diameter: 100–200 μm) were deposited on the glass surface equidistantly until the pipette was empty. The microscope was then switched to confocal fluorescence mode for time-lapse imaging.

5. Image Analysis

Image processing and analysis was performed using Fiji (ImageJ). Stack files had a multidimensional format containing image information recorded in three domains: time, Z-space and emission wavelength. For image processing the stacks were maximum-projected in Z where necessary, concatenated in time, merged to RGB color representation and saved in one single movie. Additional processing, such as distance measurements, and editing, such as labeling and scale bar addition, were performed using Fiji macros. Finally, single snapshots were saved as JEPG format files and videos as AVI format files.

III. RESULTS AND DISCUSSION

1. Studying meiosis resumption in non-fertilized eggs

Oogenesis has been extensively studied and described in considerable detail (Bastock and St Johnston 2008). Subsequent events occurring during egg activation, such as female meiosis resumption, are not well understood. In the past, developmental biologists have guided their studies either by using immunostaining (Heifetz, Yu, and Wolfner 2001) or by performing live imaging of oocytes (Endow and Komma 1997). However, both approaches relied on *in vitro* activated oocytes harvested from the female ovaries. The collection of non-fertilized egg can be achieved by performing the egg-laying assay (see Methods) or by manually dissecting eggs from the uterus of female flies. The two methods were tested; overall, egg-laying was more efficient in terms of number and developmental stage of eggs.

1.1 *In vivo* imaging of meiosis completion in *Dmel* non-fertilized egg

A protocol was established with the aim of collecting non-fertilized eggs undergoing meiosis II. Due to the lack of any specifications and temporal correlations between fertilization, meiosis completion and oviposition, the protocol was developed on the basis of an assay for early embryo collection (Telley et al. 2013). A set of factors including the number and the age of virgins, the time for egg synchronization (e.s), i.e. the

repeated exchange agar plates, and the egg collection time (e.c) was optimized in an iterative way. *In vivo* imaging of the collected non-fertilized eggs led to the observation of rosettes and a tandem pair of spindles. Both these meiotic structures were indicators that meiosis had been resumed prior to egg collection (Heifetz, Yu, and Wolfner 2001; Page and Orr-Weaver 1997). Fluorescence microscopy imaging of metaphase II spindles allowed to visualize microtubule and chromatin dynamics during meiosis completion. The spindles were initially interconnected by one of their poles with the chromatin tightly packed at the metaphase plate. The following meiotic stages included the individualization of the two meiotic spindles and the formation of the four pronuclei (Figure 1).

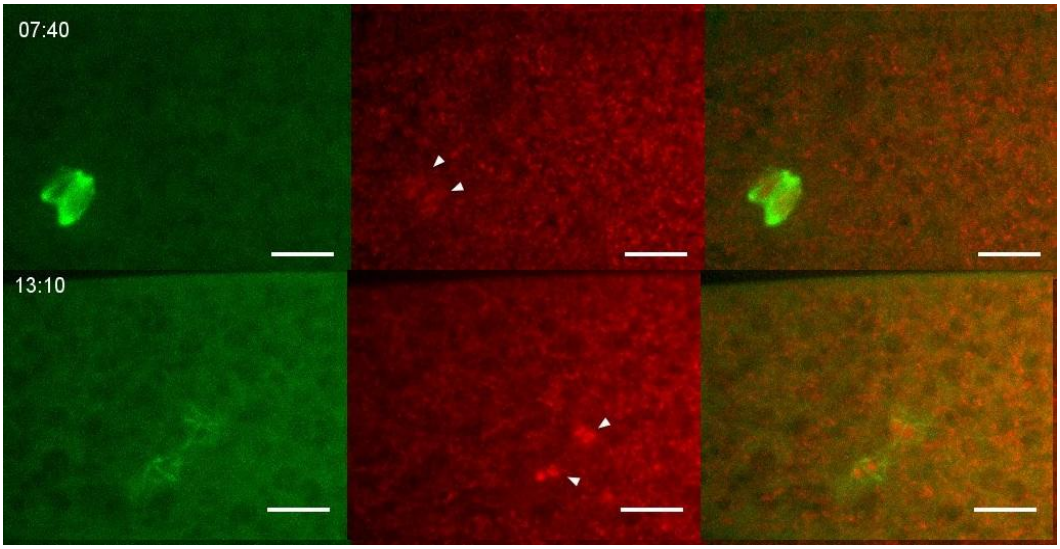

Figure 1 - Time-lapse sequence of top-view images from a non-fertilized egg undergoing meiosis completion. (**Time 07:40**) In a jackknife movement, the two spindles overlapped and the condensed chromatin moved towards the poles of each spindle. Microtubule depolymerization was identified at the spindle midzone. (**Time 13:10**) The final four products of meiosis moved towards the center of the egg and remained grouped (arrowheads). A microtubule network formed around each set of two pronuclei. Microtubules are in green (Jup::GFP), left column. Chromatin is in red (His2Av::RFP), middle column. Both colors merged, right column. Scale bar, 20 µm.

2. *Ex vivo* isolation of pronuclei from fertilized eggs

For the reconstitution of fertilization, a novel assay was developed with the aim of providing *ex vivo* live imaging capability of events following sperm activation. Both *in vivo* and *ex vivo* conditions combined with live microscopy were realized, allowing time-lapse visualization of two processes naturally occurring deep inside the egg, pronuclear apposition and the first mitotic nuclear division. However, *in vivo* imaging suffered from known technical limitations (e.g. low penetration depth and detail). The protocol followed for the collection of non-fertilized eggs gave important insight into the developmental timing of eggs, and this information helped defining the protocol to obtain eggs at this very early stage of fertilization. Due to the lack of temporal

evidence for processes occurring after sperm entry into the egg, two different strategies were followed when collecting eggs where sperm had just entered. These included harvesting eggs by manually dissecting eggs from mated females or by performing the egg-laying assay. Similar as in the last section the egg-laying assay was more efficient for the collection of recently fertilized eggs in terms of number and stage of development.

2.1 First *in vivo* evidence of pronuclear apposition in recently fertilized eggs

Following Protocol 4 (see Appendix) enabled for the first time the visualization of the pronuclear apposition in a recently fertilized egg. Initially, a single pronucleus was visualized close to the center of the egg, with the chromatin decondensed and surrounded by a bright radial array of microtubules (Figure 2; time 00:35). As the chromatin started to condense, the microtubule network seemed to disperse in the cytoplasm (Figure 2; time 03:50). Finally, two separate masses of chromatin appeared at the same focal level, surrounded by a dense array of microtubules (Figure 2; time 08:10). Because it was not implemented a centrosomal marker in the experiments, these images were not conclusive in whether the first pronucleus identified was the female or the male. However, it was speculate that it was indeed the male pronucleus for the following reasons. Firstly, it was associated with an MTOC and surrounded by a radial array of microtubules. Secondly, no polar body was detected at the cortex facing the glass, suggesting that the female pronucleus must have been on the distal side relative to the glass and objective. This suggests a nuclear configuration where the male nucleus is stationary and the female pronucleus is moving towards the focal plane. The microtubule array visible could play a role in the migration of the female pronucleus.

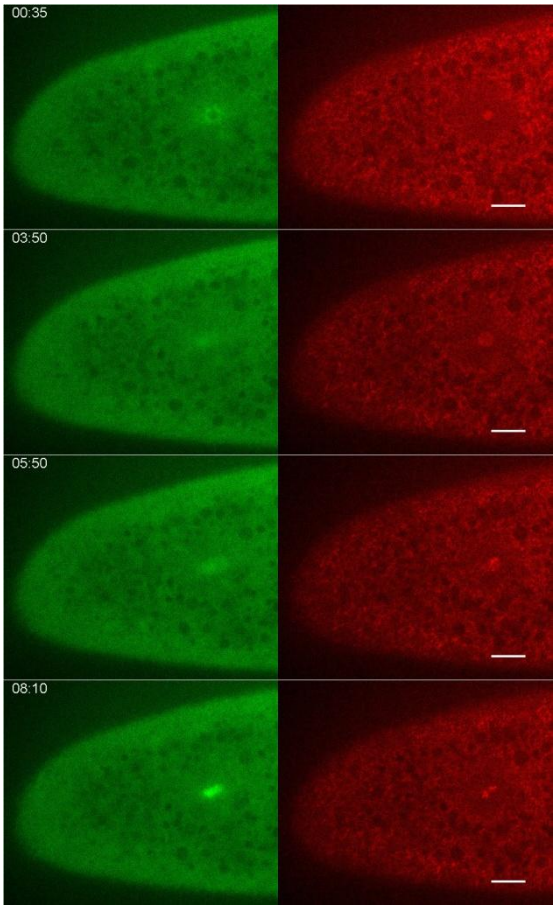

Figure 2 – Single plane time-lapse images of pronuclear apposition in a recently fertilized egg. **(Time 00:35)** A single pronucleus was located close to the center of the egg and exhibited a not very dense but radial array of microtubules surrounding the nucleus. **(Time 03:50)** The chromatin decondenses and the pronucleus enlarges. The microtubule array disperses in the cytoplasm. **(Time 05:50)** The chromatin condenses in the nucleus, and the microtubule array reorganizes. **(Time 08:10)** A second, distinct chromatin mass appears, but does not fuse with the initial chromatin mass. The array of microtubules increases in density and forms a barrel shape. Red marks chromatin (His2Av::RFP) and green marks microtubules (Jup::GFP). Scale bar, 20 µm.

Note that this interpretation is in line with an earlier proposed model in which the sperm aster traps the female pronucleus and mediates the migration of the female towards the male pronucleus (Callaini and Riparbelli 1996). Further experiments in a reduced volume and with a centrosomal marker for overall better imaging are necessary to clarify the causality of pronuclear migration.

2.2 *Ex vivo* extract of eggs in pronuclear apposition

Eggs that were laid shortly before their collection, and that showed a single nucleus (Figure 3; time 00:35) according to the egg laying scheme described above, were considered to be undergoing pronuclear apposition. These eggs were chosen for pipette-based extraction of the cytoplasmic content (Telley et al. 2013). The sperm tail was not always detected inside the intact egg. However, it was readily visible in the cytoplasm droplet after extraction (Figure 3), confirming that the egg was indeed fertilized. In one particular example of extraction, a network of microtubules polymerized around seemingly two sets of condensed chromatin (Figure 3; time 00:00 and inset). Subsequently, a barrel-shaped microtubule structure closely resembling a spindle self-assembled while the chromatids were aligned at the equatorial region (Figure 3; time 00:30). Considering that the extraction was performed on a fertilized egg, one would assume that this

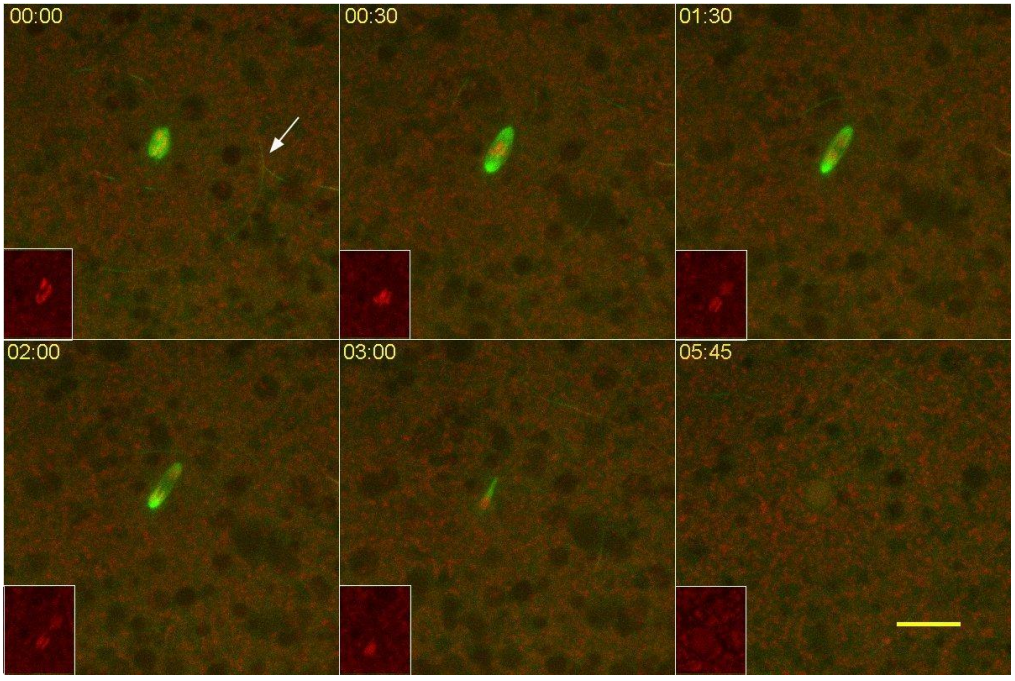

Figure 3 - First sequence of fluorescence time-lapse images of a droplet of cytoplasm extracted from an egg undergoing pronuclear apposition before extraction. **(Time 00:00)** A microtubule network formed around two separate groups of condensed chromatin. The sperm tail was visualized in the cytoplasm droplet (arrow). **(Time 00:30)** The chromatin is tightly packed at the equatorial region of an anastral spindle-like structure. **(Time 01:30)** As the two contents of condensed chromatin migrate towards the poles of the spindle, microtubule depolymerization starts at the equatorial plane. **(Time 02:00)** Once at the poles, chromatin decondenses, alongside with microtubule depolymerization. **(Time 03:00)** Only one daughter nucleus remains in the focal plane. **(Time 05:45)** The focused nucleus enlarges. Chromatin decondenses and microtubules disperse in the cytoplasm. Red marks chromatin (His2Av::RFP) and green marks microtubules (Jup::GFP). Scale bar, 20 µm.

was a mitotic spindle in metaphase. However, contrary to what was described by Riparbelli and Callaini (1996) this spindle seemed to be anastral, devoid of microtubules nucleated at the poles. Despite the absence of astral microtubules, the spindle elongated and the chromatids started to move towards the poles in separate groups (Figure 3; time 01:30), corresponding to the transition from metaphase to anaphase. Then, chromatid decondensation was concomitant with microtubule depolymerization at the equatorial region (Figure 3; time 02:00). Presumably, at the beginning of telophase one of the daughter nuclei left the focal volume (Figure 3; time 03:00). In the subsequent interphase, chromatin decondensation was concomitant with an increase in size of the daughter nucleus in focus (Figure 3; time 05:45). *In vivo* imaging of eggs in pronuclear apposition led to the observation of a similar nuclear behavior for spindles looking to be anastral. The absence of astral microtubules at the poles of the spindle raised the question of categorizing this process as being the first mitotic division. Despite the absence of the sperm tail in the cytoplasm, no tandem pair of meiotic spindles or rosette were observed. The presence of the sperm tail in the extract suggested that the egg was indeed fertilized. To further support the notion of a mitotic division, the diameter of one of the daughter nuclei was estimated and compared to the study of mitotic nuclear divisions in *Dmel* embryo extracts. During mitosis, the diameter of a nucleus at early interphase is ~6 µm and grows to ~8 µm by late interphase (Telley et al. 2012) (I.A. Telley, pers. communication). The chromatin area was estimated for one of the two nuclei in the droplet throughout the division between time points 00:00 and 06:00. The diameter of the nucleus at mid-to-late interphase was estimated ~7 µm, assuming circular geometry, which is consistent with the values measured in later syncycial mitotic divisions. One possible explanation for the absence of centrosomes in the extract would be the frequently observed dissociation of centrosomes or spindle pole from the nuclei during extraction of *Dmel* embryos (Telley et al. 2013) Furthermore, it has been described in the literature that microtubule nucleation during spindle formation can occur even in the absence of functional centrosomes (Bonaccorsi, Giansanti, and Gatti 2000; Debec et al. 1995; Heald and Tournebize 1996; Megraw et al. 1999).

IV. CONCLUSIONS

During the course of this thesis, the main technical approaches were derived from a novel single-embryo *ex vivo* assay. At the core of this method are an egg laying assay to retrieve embryos in a particular developmental stage, and a micro-manipulation confocal microscope allowing extraction and time-lapse imaging of nucleus-cytoplasm. This assay was suitable for the egg extract and the sperm micromanipulation. *In vivo* imaging of non-fertilized eggs allowed to visualize for the first time meiosis II completion in naturally activated eggs. Additional understanding of the role of

distinct centrosomal components in the assembly and maintenance of the tandem pair of spindles is needed. *In vivo* and *ex vivo* imaging of eggs undergoing pronuclear apposition brought new temporal and dynamics insights of chromatin and microtubule cytoskeleton during pre-mitotic phases. However, the resolution of and the details gained from *in vivo* imaging were limited and, thus, volume reduction through extraction was performed. For both cases the dynamics of the centrioles and centrosomes in recently fertilized eggs should to be more accurately addressed in a fly strain expressing centrosome markers, such as centrosomin (Cnn). The position of the centrosomes during pronuclear apposition will help distinguishing between the male and the female pronucleus, identifying the moment of centrosome replication during the formation of the sperm aster, and monitoring the assembly of the first zygotic centrosome. Once optimized, some of the protocols developed can be applied as tools for applications such as the study of cytoplasmic incompatibility in *Wolbachia*-infected eggs.

REFERENCES

1. Bastock, Rebecca, and Daniel St Johnston. 2008. "Drosophila Oogenesis." *Current biology : CB* 18(23): R1082–87.
2. Bonaccorsi, S, M G Giansanti, and M Gatti. 2000. "Spindle Assembly in Drosophila Neuroblasts and Ganglion Mother Cells." *Nature cell biology* 2(1): 54–56.
3. Callaini, G, and M G Riparbelli. 1996. "Fertilization in Drosophila Melanogaster: Centrosome Inheritance and Organization of the First Mitotic Spindle." *Developmental biology* 176(2): 199–208.
4. Debec, A et al. 1995. "Polar Organization of Gamma-Tubulin in Acentriolar Mitotic Spindles of Drosophila Melanogaster Cells." *J. Cell Sci.* 108(7): 2645–53.
5. Endow, SA, and DJ Komma. 1997. "Spindle Dynamics during Meiosis in Drosophila Oocytes." *The Journal of cell biology* 137(6): 1321–36.
6. Fitch, KR, and GK Yasuda. 1997. "1 Paternal Effects in Drosophila: Implications for Mechanisms of Early Development." *Current topics in …* 38: 1–34.
7. Foe, VE, and BM Alberts. 1983. "Studies of Nuclear and Cytoplasmic Behaviour during the Five Mitotic Cycles That Precede Gastrulation in Drosophila Embryogenesis." *Journal of cell science* 61(1): 31–70.
8. Heald, R, and R Tournebize. 1996. "Self-Organization of Microtubules into Bipolar Spindles around Artificial Chromosomes in Xenopus Egg Extracts." *Nature* 382(6590): 420–25.
9. Heifetz, Y, J Yu, and M F Wolfner. 2001. "Ovulation Triggers Activation of Drosophila Oocytes." *Developmental biology* 234(2): 416–24.
10. Megraw, TL, K Li, LR Kao, and TC Kaufman. 1999. "The Centrosomin Protein Is Required for Centrosome Assembly and Function during Cleavage in Drosophila." *Development* 126(13): 2829–39.
11. Page, A W, and T L Orr-Weaver. 1997. "Activation of the Meiotic Divisions in Drosophila Oocytes." *Developmental biology* 183(2): 195–207.
12. Perotti, M.E. 1975. "Ultrastructural Aspects of Fertilization in Drosophila." *International Symposium on the Functional Anatomy of the Spermatozoon*.
13. Riparbelli, MG, and G Callaini. 1996. "Meiotic Spindle Organization in Fertilized Drosophila Oocyte: Presence of Centrosomal Components in the Meiotic Apparatus." *Journal of cell science* 109(5): 911–18.
14. Sonnenblick, BP. 1950. "The Early Embryology of Drosophila Melanogaster." *Biology of Drosophila*: 62–167.
15. Telley, Ivo A, Imre Gáspár, Anne Ephrussi, and Thomas Surrey. 2012. "Aster Migration Determines the Length Scale of Nuclear

Separation in the Drosophila Syncytial Embryo." *The Journal of cell biology* 197(7): 887–95.
16. Telley, Ivo A, Imre Gáspár, Anne Ephrussi, and Thomas Surrey. 2013. "A Single Drosophila Embryo Extract for the Study of Mitosis Ex Vivo." *Nature protocols* 8(2): 310–24.
17. Zalokar, M, and I Erk. 1976. "Division and Migration of Nuclei during Early Embryogenesis of Drosophila Melanogaster." *Journal de microscopie et de biologie cellulaire*.

APPENDIX

Protocol 4 was continuously redefined by testing different combinations of durations for e.s and e.c. Three different timing schemes were defined and tested (Table 1). The final scheme T_3 allowed to collect eggs at the earliest stages of fertilization.

Table 1 – A series of different timing schemes was tested for the collection of fertilized eggs in that were in a pre-mitotic stage. Each combination includes the timing for egg synchronization (e.s), egg collection (e.c) and the average time for egg preparation (e.p).

Timing scheme (T_i, $i \in \{1,2,3\}$)	**e.s (min)**	**e.c (min)**	$\overline{\textbf{e.p}}$ **(min)**
T_1	3x15	10	6
T_2	3x10	[8,5]	6
T_3	3x10	7-6	5.5